International Journal for Parasitology: Parasites and Wildlife 23 (2024) 100905

Contents lists available at ScienceDirect

International Journal for Parasitology: Parasites and Wildlife

journal homepage: www.elsevier.com/locate/ijppaw

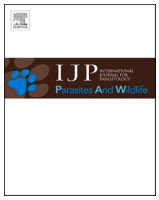

Unexpected absence of exo-erythrocytic merogony during high gametocytaemia in two species of *Haemoproteus* (Haemosporida: Haemoproteidae), including description of *Haemoproteus angustus* n. sp. (lineage hCWT7) and a report of previously unknown residual bodies during in vitro gametogenesis

Gediminas Valkiūnas [a,*], Tatjana Iezhova [a], Mikas Ilgūnas [a], Mélanie Tchoumbou [a], Mélanie Duc [a], Dovilė Bukauskaitė [a], Tanja Himmel [b], Josef Harl [b], Herbert Weissenböck [b]

[a] *Nature Research Centre, Akademijos 2, 08412, Vilnius, Lithuania*
[b] *Institute of Pathology, Department for Biological Sciences and Pathobiology, University of Veterinary Medicine Vienna, Veterinaerplatz 1, 1210, Vienna, Austria*

ARTICLE INFO

Keywords:
Avian haemosporidian parasites
New species
Tissue merogony
In vitro gametogenesis
Chromogenic in situ hybridization
DNA haplotype network

ABSTRACT

Neglected avian blood parasites of the genus *Haemoproteus* (Haemoproteidae) have recently attracted attention due to the application of molecular diagnostic tools, which unravelled remarkable diversity of their exo-erythrocytic (or tissue) stages both regarding morphology and organ tropism levels. The development of haemoproteids might result in pathologies of internal organs, however the exo-erythrocytic development (EED) of most *Haemoproteus* species remains unknown. Seven individual birds - *Curruca communis* (1) and *Phylloscopus trochilus* (6) – with high gametocytaemia (between 1% and 24%) of *Haemoproteus angustus* n. sp. (hCWT7) and *Haemoproteus palloris* (lineage hWW1) were sampled in Lithuania, and their internal organs were examined extensively by parallel application of histology and chromogenic in situ hybridization methods. Tissue stages were apparently absent, suggesting that the parasitaemia was not accompanied by detectable tissue merogony. *Haemoproteus angustus* n. sp. was described and characterized morphologically and molecularly. Sexual process and ookinete development of the new species readily occurred in vitro, and a unique character for *Haemoproteus* parasites was discovered – the obligatory development of several tiny residual bodies, which were associated with intracellular transformation of both macrogametocytes and microgametocytes before their escape from the host cells and formation of gametes. A DNA haplotype network was constructed with lineages that cluster in one clade with the lineage hCWT7. This clade consists of lineages mostly found in *Curruca* birds, indicating specificity for birds of this genus. The lineage hCWT7 is mainly a parasite of *C. communis*. Most reports of this lineage came from Turkey, with only a few records in Europe, mostly in birds wintering in Africa where transmission probably occurs. This study highlights unexpected difficulties in the research of EED even when using sensitive molecular diagnostic tools and extends information about transformation in early stages of gametogenesis in haemosporidian parasites.

1. Introduction

Haemoproteus (Haemoproteidae) parasites are cosmopolitan haemosporidians (Apicomplexa, Haemosporida) that are specific bird parasites transmitted by blood-sucking dipteran insects of the families Ceratopogonidae and Hippoboscidae (Valkiūnas and Atkinson, 2020). Sporozoites initiate the development of tissue stages or exo-erythrocytic stages (meronts and/or megalomeronts) in avian hosts. Merozoites develop in the latter two tissue stages. When mature, the merozoites invade red blood cells and produce gametocytes, the intracellular stage

* Corresponding author.
E-mail addresses: gediminas.valkiunas@gamtc.lt (G. Valkiūnas), tatjana.jezova@gamtc.lt (T. Iezhova), ilgunasmikas@gmail.com (M. Ilgūnas), melanie.tchoumbou@gamtc.lt (M. Tchoumbou), Melanie.Duc@gamtc.lt (M. Duc), dovile.bukauskaite@gamtc.lt (D. Bukauskaitė), Tanja.Himmel@vetmeduni.ac.at (T. Himmel), Josef.Harl@vetmeduni.ac.at (J. Harl), Herbert.Weissenboeck@vetmeduni.ac.at (H. Weissenböck).

https://doi.org/10.1016/j.ijppaw.2024.100905
Received 10 December 2023; Received in revised form 6 January 2024; Accepted 6 January 2024
Available online 9 January 2024

infective for insect vectors, in which the sporogonic development takes place. The produced sporozoites are the stage responsible for infection of new avian hosts. This basic scheme of the *Haemoproteus* spp. life cycle is obvious, but details of the development remain insufficiently investigated in most described parasite species. For example, it remains unclear if megalomeronts (huge-sized tissue stages) develop in all *Haemoproteus* species and what is their relationship with meronts (small-sized tissue stages) during development in birds (Duc et al., 2023a, 2023b; Himmel et al., 2024). These issues are important for better understanding the mechanisms of pathologies during avian haemoproteosis.

Haemoproteus parasites were largely neglected in veterinary medicine due to a predominant belief about their harmlessness in avian hosts (Valkiūnas and Iezhova, 2017). Several early studies described avian pathologies associated with tissue stages of unidentified haemosporidians, which probably were megalomeronts of *Haemoproteus* parasites (Borst and Zwart, 1972; Fowler and Forbes, 1972; Smith, 1972; Walker and Garnham, 1972; Gardiner et al., 1984; Earlé et al., 1993). However, these were mainly case reports based solely on microscopic examinations, which revealed tissue stages whose morphology was atypical for haemosporidian parasites. Consequently, these findings were questioned and assumed to relate to other apicomplexan protists (Bennett et al., 1993). Recent molecular studies, and particularly the application of chromogenic in situ hybridization (CISH) diagnostic methods, which use genus- and species-specific probes targeting the parasites' RNA, have proved that tissue stages of *Haemoproteus* parasites are remarkably diverse and are responsible for the damage of various internal organs (Ilgūnas et al., 2019; Himmel et al., 2019, Himmel et al., 2024; Duc et al., 2023a, 2023b). Marked damage of lungs, heart, brain, and many other organs by *Haemoproteus* spp. exo-erythrocytic stages hardly can be considered as benign in affected hosts (Ortiz-Catedral et al., 2019; Hernández-Lara et al., 2021; Duc et al., 2023a, 2023b; Himmel et al., 2024; Cococcetta et al., 2023). Nevertheless, the virulence and patterns of exo-erythrocytic development remain only fragmentally investigated in haemoproteids and remain unassessed in most described species (Valkiūnas and Iezhova, 2017; Duc et al., 2023a, 2023b; Himmel et al., 2024). These are obstacles to better understand the general patterns of exo-erythrocytic development in haemoproteids, particularly for unravelling the question if the development of both meronts and megalomeronts is obligatory for each *Haemoproteus* species or if these different tissue stages occur independently in some parasite species.

As a part of ongoing projects on mechanisms of exo-erythrocytic development of avian haemoproteids, this study examined two species of naturally infected birds – the common whitethroat *Curruca communis* and the willow warbler *Phylloscopus trochilus* – with high gametocytaemia of *Haemoproteus* sp. (lineage hCWT7) and *Haemoproteus palloris* (hWW1), respectively. Both host species are common Palearctic migratory birds wintering in sub-Saharan Africa (Svensson, 1992; Snow and Perrins, 1998; Bensch and Åkesson, 2003). The main aim was to examine organs of the infected birds for tissue stages and to determine which tissue stages were associated with different parasite species present in high parasitaemia in different parasite species. Further, this study aimed to provide morphological and molecular description of a new *Haemoproteus* species, *Haemoproteus angustus* n. sp. (hCWT7), with analysis of its phylogenetic relationships and geographic and host distribution using DNA haplotype networks.

2. Materials and methods

2.1. Study site and sampling

The material was collected at the Ventės Ragas Ornithological Station, Lithuania (55°21′ N, 21°12′ E) during spring migration (May) in 2015, 2017 and 2019. In all, 53 individual common whitethroats *Curruca communis* were caught and their blood films were examined microscopically. Approximately 50 µl of blood were collected in heparinized microcapillaries by puncturing the brachial vein. Blood films were prepared on ready-to-use glass slides immediately after withdrawal; they were quickly dried using a battery-operated fan, fixed in absolute methanol for 1 min and stained with Giemsa using the standard protocol (Valkiūnas, 2005). The remaining blood was fixed in SET-buffer (Hellgren et al., 2007) for molecular analysis, maintained at +4 °C in the field and −20 °C in the laboratory.

As a part of the fieldwork, blood and tissue samples from six willow warblers with *Haemoproteus palloris* (lineage hWW1; parasitaemia ranging between 8% and 24%) were collected for histological examination of organs aiming to detect tissues stages of this parasite. The infected birds were selected for histological investigation in the field using a protocol described by Valkiūnas et al. (2016). Briefly, one methanol-fixed blood film was stained with Giemsa solution (30%) for 15 min and quickly scanned microscopically at high magnification (1000×) by examination of approximately 20 visual fields aiming to select intensively infected bird individuals. Intensity of infection was estimated as a percentage by counting the number of parasites per 1000 red blood cells. Species of *Haemoproteus* were identified according to Valkiūnas (2005) and Dimitrov et al. (2016).

In all, seven infected birds – one common whitethroat and six willow warblers – were euthanized for histology, and additional blood films (about 10–15) were prepared for taxonomic collection purposes as described above. The brain, heart, lungs, liver, kidneys, pectoral and leg muscles, and spleen were collected from the birds sacrificed in 2017, and the trachea oesophagus, gizzard, intestine, and reproductive organs were additionally collected from the birds sacrificed in 2019. Organs were fixed and processed for histological examination (see description of histological methods below). Organ samples of common whitethroat and willow warblers were examined in Vienna and Vilnius, respectively. From birds collected in 2015, the organs were unavailable for investigation, and only blood films were examined.

2.2. Microscopic examination and parasite morphology

Several models of Olympus light microscopes were used for examination of blood films and in vitro preparations of the parasites in the field and laboratory. The Olympus BX61 microscope equipped with an Olympus DP70 digital camera and the imaging software AnalySIS FIVE (Olympus, Tokyo, Japan) were used for preparation of parasite illustrations and parasite measurements. Morphology of the blood stages of the new species was compared with morphologically similar *Haemoproteus* parasites of passeriform birds using the parasites' type or voucher specimens. These were *Haemoproteus belopolskyi* (accession no. type/voucher: 435.85/49698 NS), *Haemoproteus dolniki* (1178.90/49699 NS), *Haemoproteus homogeneae* (49064 NS/49700 NS), *Haemoproteus majoris* (49701 NS), *Haemoproteus pallidulus* (5420 NS/49702 NS), *Haemoproteus parabelopolskyi* (15317 NS/49703 NS), and *Haemoproteus sittae* (49704 NS) deposited in the Collection of Nature Research Centre (NRC), Lithuania. Student's *t*-test for independent samples was used to determine statistically significant differences between mean linear parameters of gametocytes and their host cells. A *P*-value of 0.05 or less was considered significant.

2.3. In vitro gametes, zygotes and ookinetes

One common whitethroat naturally infected with *H. angustus* n. sp. was used as a donor of mature gametocytes for in vitro observation of the exflagellation, gametes, zygotes and ookinetes. The method described by Valkiūnas et al. (2021) was used to access these parasite stages. Briefly, approximately 300 µl of blood were taken from the brachial vein, immediately placed in 2 ml Eppendorf tubes and diluted with 3.7% solution of sodium citrate at a ratio of 1 part of the solution to 4 parts of blood. To prevent the solution with blood from drying out, each Eppendorf tube was placed in a polypropylene container (60 ml) with a cap and a sheet of moist filter paper in the bottom. The mixture

was stirred gently using a small glass stick, and blood films were prepared at time points of 1, 3, 5, 10, 15, 30 and 45 min and at 1, 2, 3, 4, 6, 8, 10, 12, 16 and 24 h after exposure of blood to air (EBA). They were air-dried, fixed in methanol, stained with Giemsa and examined under the microscope, as blood films. The work was performed at 20 ± 1 °C. Representative preparations of microgametes, macrogametes, zygotes and ookinetes were deposited in the Nature Research Centre, Vilnius, Lithuania (see parasite description).

2.4. Histological examination

Tissue samples of the common whitethroat were examined in Vienna. The organs were fixed in 10% neutral buffered formalin solution (pH 7.4) for approximately 24 h at room temperature. After washing in distilled water for 15 min, samples were dehydrated through a series of graded ethanol (70%, 96%, 100%), cleared in xylene, and embedded in paraffin wax. Formalin-fixed paraffin-embedded (FFPE) tissue blocks were cut with a microtome, and 2 μm thick sections were prepared according to the following procedure. In the first round, of each organ 60 serial sections were cut, which alternately were subjected to haematoxylin-eosin (HE) staining and chromogenic in situ hybridization (CISH). After the first 60 sections, each two serial sections (one for HE-staining, the other for CISH) were prepared at intervals of 100 μm until the blocks were entirely cut. In total, 96 sections of each FFPE-block (hence 96 sections of each organ) were prepared (48 for HE and 48 for CISH). Tissue sections were mounted on regular glass slides for HE-staining, and on SuperFrost Plus Adhesion slides (Epredia, Portsmouth, USA) for CISH, and immediately air-dried. HE-stained sections and sections treated with CISH were screened for exo-erythrocytic tissue stages at 100x and 200x magnifications using an Olympus light microscope.

Tissue stages of willow warbles were examined in Vilnius using a similar protocol, with minor differences. Briefly, tissue samples were fixed in 10% neutral buffered formalin solution (pH 7.4) for 24 h at ambient temperature. The samples were dehydrated with ethanol, transferred to isopropanol, and embedded in paraffin wax. FFPE tissue blocks were cut with a microtome and 3 μm thick sections were prepared. Nine slides for HE-staining and one slide for CISH were prepared repeatedly till the blocks were cut entirely. Roughly, 2 to 4 sections were placed on each glass slide. In total (counting sections of different organs together), 1952 sections were prepared (for 1803 HE and for 149 CISH) and examined under 40x, 100x, 200x and 400x.

2.5. Chromogenic in situ hybridization

CISH was performed following a previously established protocol using a *Haemoproteus*-specific oligonucleotide probe (Haemo18S, sequence: 5′-GCTAACCGTAGT TATAGTCGCCATCTC-3′) targeting the *18S* ribosomal RNA of parasites of the subgenus *Parahaemoproteus* (Himmel et al., 2019). It was proved to be sensitive in the diagnostics of tissue stages of the parasites in several recent studies (Duc et al., 2023a, 2023b; Himmel et al., 2024). Briefly, FFPE tissue sections were deparaffinized and pre-treated with proteinase K (Roche, Basel, Switzerland) 3 μg/ml for 40 min at 37 °C. After proteolysis, sections were rinsed in distilled water, dehydrated for 5 min each in 90% and 100% ethanol, and air-dried. Next, tissue sections were covered with the hybridization mixture containing 1 ng/100 μl digoxigenin-labelled Haemo18S probe, and incubated overnight at 40 °C. After hybridization, sections were subjected to stringency washes in SSC solutions and subsequently incubated with anti-digoxigenin-AP Fab fragments (Roche) at a concentration of 1:200 for 1 h. After a washing step, sections were incubated with the chromogenic substrates 5-bromo-4-chloro-3-indolyl phosphate (BCIP) and 4-nitro blue tetrazolium chloride (NBT) (Roche) for 1.5 h in a dark chamber to allow formation of a dark purple precipitate and visualization of parasite-probe hybrids. Finally, sections were rinsed in TE-buffer, counterstained with haematoxylin, and covered with Aquatex (Merck, Darmstadt, Germany) and glass coverslips. For each CISH procedure (processing approximately 15 slides), a positive control slide containing tissue samples of birds previously determined CISH-positive for *Haemoproteus* parasites was included.

2.6. Deoxyribonucleic acid extraction, polymerase chain reaction and sequencing

Total DNA was extracted from whole blood using the standard ammonium acetate DNA precipitation protocol (Sambrook and Russel, 2001). Molecular diagnostics and identification of genetic lineages was carried out by application of a nested PCR protocol using the primer pairs HaemNFI/HaemNR3 and HaemF/HaemR2 (Bensch et al., 2000; Hellgren et al., 2004), amplifying a 478 bp fragment of the cytochrome *b* gene (*cytb*). Conditions for all reactions were maintained as in the original protocol. In short, the extracted DNA was diluted to 25 ng/μl and used as a template for first reaction of the nested PCR protocol. The product of the first PCR reaction was used as the template for the second step. PCRs were carried out in 25 μl reaction volumes comprised of 12.5 μl of DreamTaq Master Mix (Thermo Fisher Scientific, Vilnius, Lithuania), 8.5 μl of nuclease-free water, 1 μl of each primer and 2 μl of template DNA per sample. A *Haemoproteus* sp.-positive sample and ddH_2O were used as positive and negative controls, respectively every 8 samples to rule out possible contaminations and evaluate the success of the PCR. Electrophoresis on a 2% agarose gel using 1 μl of the final PCR product was performed to check for positive amplification. Successfully amplified fragments were sequenced using the Big Dye Terminator V3.1 Cycle Sequencing Kit and ABI PRISMTM 3100 capillary sequencing robot (Applied Biosystems, Foster City, CA, USA). The obtained sequences were analysed using the Geneious Prime 2022.1.1 (https://www.geneious.com, accessed on May 12, 2022) software. They were deposited in GenBank (OQ383418, OR8232030).

2.7. Phylogenetic analysis

A Bayesian phylogenetic tree was constructed using 61 *Haemoproteus* and four *Plasmodium* lineages, with one *Leucocytozoon* lineages used as outgroup. The tree only contains *Haemoproteus* parasite mitochondrial *cytb* gene sequences of morphologically identified parasites, which were selected based on the recent review (Valkiūnas and Iezhova, 2022). Lineages covering at least 464 bp length fragments of the *cytb* gene (the barcoding sequence) were used in this analysis. The software jModeltest-2.1.10 (Guindon and Gascuel, 2003; Darriba et al., 2012) was used to select the best fitting model, which was GTR + I + G as implemented in software Geneious Prime 2022.1.1 (https://www.geneious.com, accessed on May 12, 2022) with the MrBayes plugin v3.2.6 (Huelsenbeck and Ronquist, 2001). Bayesian inference was run for 3 million generations, and sampled every 100th generation, while discarding the first 25% of trees as a 'burn-in' period for the construction of the consensus tree.

2.8. Phylogenetic tree and DNA haplotype network of cytb lineages closely related to Haemoproteus angustus n. sp. (hCWT7)

To determine the phylogenetic relationship of *H. angustus* hCWT7 with closely related *Haemoproteus* lineages, a Maximum Likelihood (ML) tree was calculated based on all barcode *Haemoproteus* lineages listed in the MalAvi database (http://130.235.244.92/Malavi/index.html, accessed November 2023) and other lineages available in NCBI GenBank, which have not been incorporated in the MalAvi database yet. The sequences were aligned with MAFFT v.7. (Katoh and Standley, 2013) applying the default option (FFT–NS–2). The sequences were collapsed to haplotypes using the online tool ALTER (Glez-Peña et al., 2010; https://www.sing-group.org/ALTER/). A ML bootstrap tree (1000 replicates) was calculated with IQ-TREE v.1.6.12 (Nguyen et al., 2015) based on a 478 bp alignment including 1546 unique *Haemoproteus* lineages

applying the substitution model GTR + I + G (tree not shown). In this ML tree, *H. angustus* hCWT7 fell into a highly supported clade featuring 21 lineages. Based on this subset of lineages, ML and BI trees were calculated using *Haemoproteus payevskyi* hRW1 (AF254968) as outgroup. A model test was performed with IQ-TREE v.1.6.12, suggesting that TN (Tamura-Nei, 1993) + G was the best-fit substitution model based on the corrected Akaike Information criterion (cAIC). A BI tree was calculated with MrBayes v.3.2 using the next best available model GTR (Generalized Time-reversible model) + G; the analysis was run for 5 million generations (2 runs each with 4 chains, one of which was heated) and every thousandth tree was sampled. The first 25% of trees were discarded as burn-in and a 50% majority rule consensus tree was calculated from the remaining 3750 trees. A ML bootstrap (1000 replicates) majority-rule consensus tree was calculated with IQ-TREE v.1.6.12 using the model TN + G.

To visualize the geographic and host distribution of *H. angustus* hCWT7 and the 20 most closely related lineages, a DNA haplotype network was calculated based on the 478 bp *cytb* barcode sequences and information from the MalAvi database and GenBank. A Median-Joining network was calculated with Network 10.2.0.0 (Fluxus Technology Ltd, Suffolk, UK) using the default settings. The networks were graphically arranged and provided with information on hosts species and geographic regions according to the United Nations geoscheme with Network Publisher v.2.1.2.5 (Fluxus Technology Ltd). The graphics were finalized with Adobe Illustrator CC v.2015 (Adobe Inc., San José, CA, USA).

Ethical statement

Blood and tissue samples were collected by licenced researchers using the procedures, which were approved by the Environmental Protection Agency, Vilnius, Lithuania (permits 2015-04-08 Nr 21, 2017-04-26 Nr. 23, 2019-04-19 Nr. 23).

3. Results

3.1. Prevalence of parasites and phylogenetic analysis

Microscopic examination showed that the overall prevalence of *H. angustus* hCWT7 in common whitethroats was 20.8% (11/53). Gametocytes of the new species (see description below) were predominantly seen in co-infection with *Haemoproteus belopolskyi*-type parasites and *Haemoproteus* sp. morphotypes. One case of infection with *H. angustus* was selected by microscopic examination; the presence of a mono-infection in this sample was supported by the retrieval of clean DNA sequences of lineage hCWT7. Intensity of parasitaemia was relatively high (1%), with a predominant (>95%) presence of advanced and fully grown gametocytes. This bird individual was used for parasite species description and histological investigation.

Extensive histological and CISH investigation of this common whitethroat – the type host of *H. angustus* n. sp. – revealed abundant blood stage signals, however, tissue stages were not found, indicating that the readily visible relatively high gametocytaemia was not accompanied by detectable exo-erythrocytic development stages. Similarly, six willow warblers with single infections and high gametocytaemia of *H. palloris* (hWW1) and predominant presence of fully grown gametocytes were examined extensively, with the same negative result for exo-erythrocytic developmental stages, while numerous gametocyte CISH signals were seen in erythrocytes in all tissue sections. Positive control slides processed along with the tissue samples under investigation were all positive, confirming that the CISH procedures were successful.

In all histologically examined birds, blood films contained mainly fully grown gametocytes, which predominated (>95%). Intracellular merozoites were not seen, and young growing gametocytes (the size of the erythrocyte nucleus) were either absent or rare, indicating the presence of advanced parasitaemia when nearly all gametocytes reached maturity.

The phylogenetic analysis readily separated the subgenera *Parahaemoproteus* (Fig. 1, clades A–D) and *Haemoproteus* (a group of lineages related to *Haemoproteus columbae*). *Haemoproteus angustus* n. sp. hCWT7 clustered within a group of morphologically well-characterised *Parahaemoproteus* species infecting and producing gametocytes exclusively in passerine bird species (Fig. 1, clade C). The most closely related described species are *H. payevskyi* hRW01, *H. parabelopolskyi* hSYAT01, and *H. homogeneae* hSYAT16, differing by 3.8%, 5.4%, and 5.6%, respectively, in the 478 bp *cytb* barcode sequence.

3.2. Description of Haemoproteus (Parahaemoproteus) angustus n. sp. (lineage hCWT7)

Type host: Common whitethroat *Curruca communis* (Latham, 1787) (Passeriformes, Sylviidae).

DNA sequences: Mitochondrial *cytb* lineage hCWT07 (478 bp, GenBank accession no. OQ383418).

Type locality: Ventė Cape, Lithuania (55°21′ N, 21°12′ E).

Site of infection: Mature erythrocytes, no other data. Exo-erythrocytic stages were not found during extensive microscopic examination of HE-stained histological sections and the application of CISH using *Haemoproteus* parasite-specific probes.

Prevalence: Overall prevalence was 11 of 53 (20.8%) in adult common whitethroats at the type locality during spring migration.

Vectors*:* Unknown. The lineage hCWT07 appeared in the clade of *Parahaemoproteus* species in the phylogenetic analysis (Fig. 1, clades A–D), indicating that this parasite is likely transmitted by *Culicoides* biting midges, as it is the case with all studied parasite species of this subgenus (Valkiūnas and Atkinson, 2020).

Type specimens: Hapantotype (gametocytes, accession nos. 49653, 49654 NS, parasitaemia intensity is ~1%, Curruca communis, May 11, 2019; gametes, accession nos. 49655–49658 NS; in vitro ookinetes, accession nos. 49659–49661 NS, other data as for gametocytes, collected by M. Ilgūnas and D. Bukauskaitė) were deposited in Nature Research Centre (NRC), Vilnius, Lithuania. Parahapantotypes (gametocytes, accession no. G466295; gametes, accessions nos. G466296–G466299; ookinetes, accessions nos. G466300–G466302; other data as for the hapantotype) were deposited in the Queensland Museum, Queensland, Australia.

Additional material: Voucher preparation: blood films (accession nos. 49662–49669 NS) and gametes and ookinetes (49670–49696 NS) were deposited in NRC, Vilnius, Lithuania.

Etymology: The species name was derived from the Latin word *angustus* (narrow); it indicates the small width of mature gametocytes, which also induce atrophy of infected erythrocytes in width. These are distinctive features of *H. angustus* n. sp. in regard of other similar haemoproteid species parasitizing Sylviidae birds (see description below).

Zoobank registration: urn:lsid:zoobank.org:pub:929F0147–969B–4BB6-A9C7–7B6A835ACC47.

Young gametocytes (Fig. 2A): The early gametocytes were seen anywhere in infected erythrocytes, they adhere to the nuclei of erythrocytes, extend longitudinally along the nuclei, but do not displace them laterally (Fig. 2A). A few small pigment granules were visible. Gametocyte outline is usually even or slightly wavy.

Macrogametocytes (Fig. 2B–H, Fig. 3A,B, Fig. 4A, Table 1): The cytoplasm is heterogenous in appearance, often contains vacuoles of variable size; volutin granules were not seen. Growing gametocytes are thin (Fig. 2B and Fig. 3A), they extend along nuclei of erythrocytes and tended to fill up the poles of erythrocytes (Fig. 2C–E). Advanced growing parasites are closely appressed to the nuclei and envelope of erythrocytes, however, the central part of the pellicle frequently does not extend to the erythrocyte envelope, causing a ‘dip’ and giving a clear dumbbell-like appearance (Fig. 2B–E, Fig. 3A, Fig. 4A). Dumbbell-shaped gametocytes are common among the growing gametocytes. The following

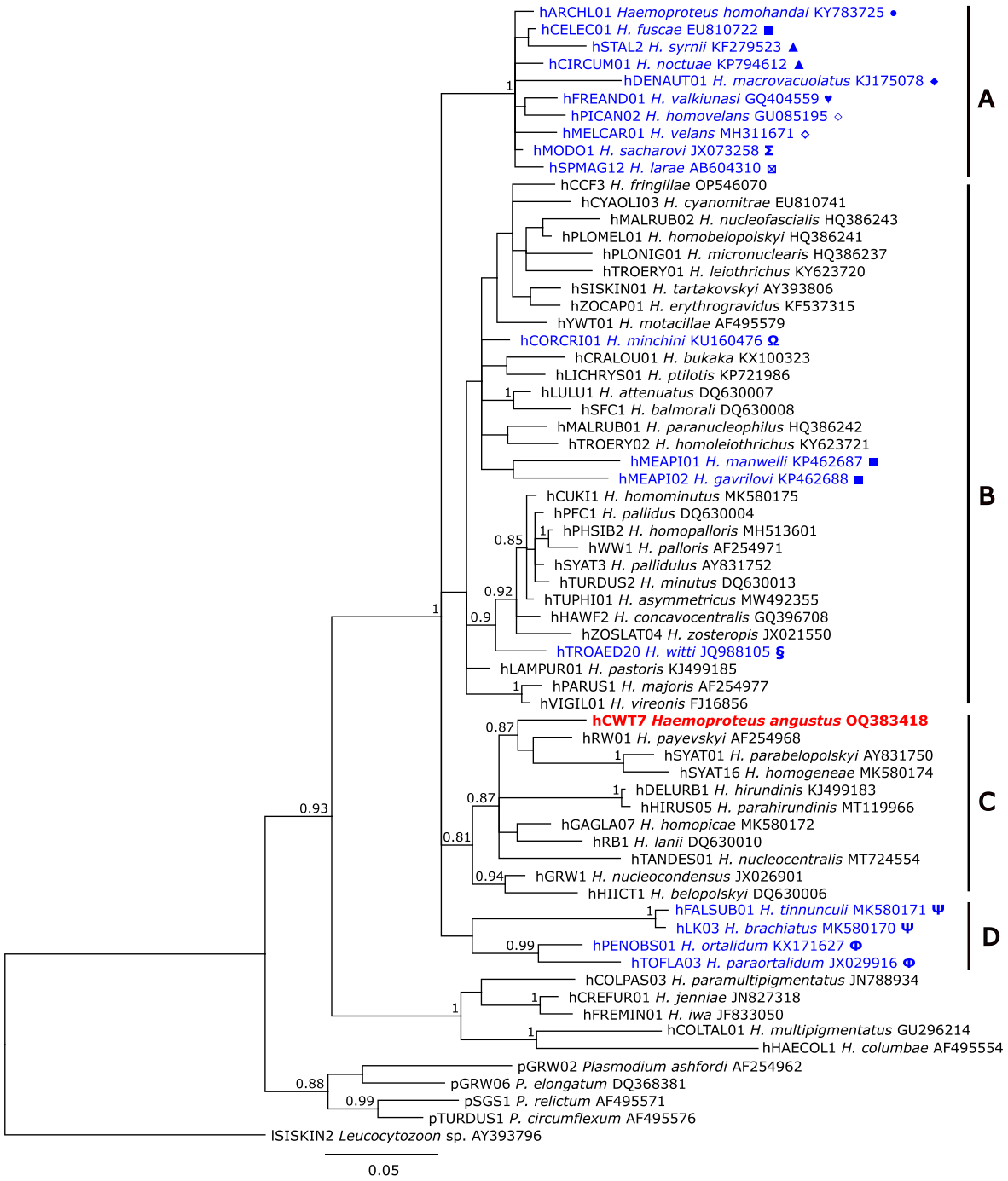

Fig. 1. Bayesian phylogenetic tree constructed using partial *cytochrome b* sequences of 61 lineages of *Haemoproteus*, 4 lineages of *Plasmodium*, and *Leucocytozoon* sp. lSISKIN2 as outgroup. Posterior probabilities higher than 0.8 are indicated close to the respective nodes. Red font indicates the parasite lineage described in this publication. Vertical bars (A–D) show groups of closely related lineages, which complete development and produce gametocytes only in non-passerines (A, D), both non-passerines and passerines (B), and only passerines (C). Blue font indicates *Haemoproteus* species, which develop in non-passerine avian hosts, which are indicated by symbols (● – Psittaciformes; ∎ - Coraciiformes; ▲ - Strigiformes; ◆ - Anseriformes; ★ - Charadriiformes; ♥ - Pelecaniformes; ⋄ - Piciformes; ⊠ - Sphenisciformes; **Ω** - Musophagiformes; § - Trochiliformes; **Ψ** – Falconiformes; **Σ** – Columbiformes; **Φ** - Galliformes). Lineage names were provided (according to MalAvi database), followed by parasite species names and sequence GenBank accession numbers.

pattern of growth of gametocytes is a characteristic feature of this species. Mainly, growth occurs by means of the obligatory attachment to the envelope of erythrocytes and the subsequent obligatory extension along the envelope, resulting in filled up poles of erythrocytes, but presence of unfilled spaces between the parasites and poles of nuclei of erythrocytes (Fig. 2B, C, F–H). The predominant growth of gametocytes along the envelope of erythrocytes in length and hardly visible growth in width, result in elongation of infected erythrocytes and their atrophy in width; these characters are readily visible in Fig. 2C–F, Fig. 3B, Fig. 4A. Fully grown gametocytes lose the dumbbell-like shape, they are closely appressed both to the nuclei and envelope of erythrocytes and fill the erythrocytes up to their poles (Fig. 2F–H, Fig. 3B). Circumnuclear gametocytes were not seen. Gametocytes frequently pull the nuclei inside (Fig. 2D, Fig. 3B and Fig. 4A), resulting in big nuclear displacement ratio (NDR), whose average value exceeds unity (see Table 1), which is a rare character of avian haemoproteids. Gametocyte outline is even (Fig. 2E

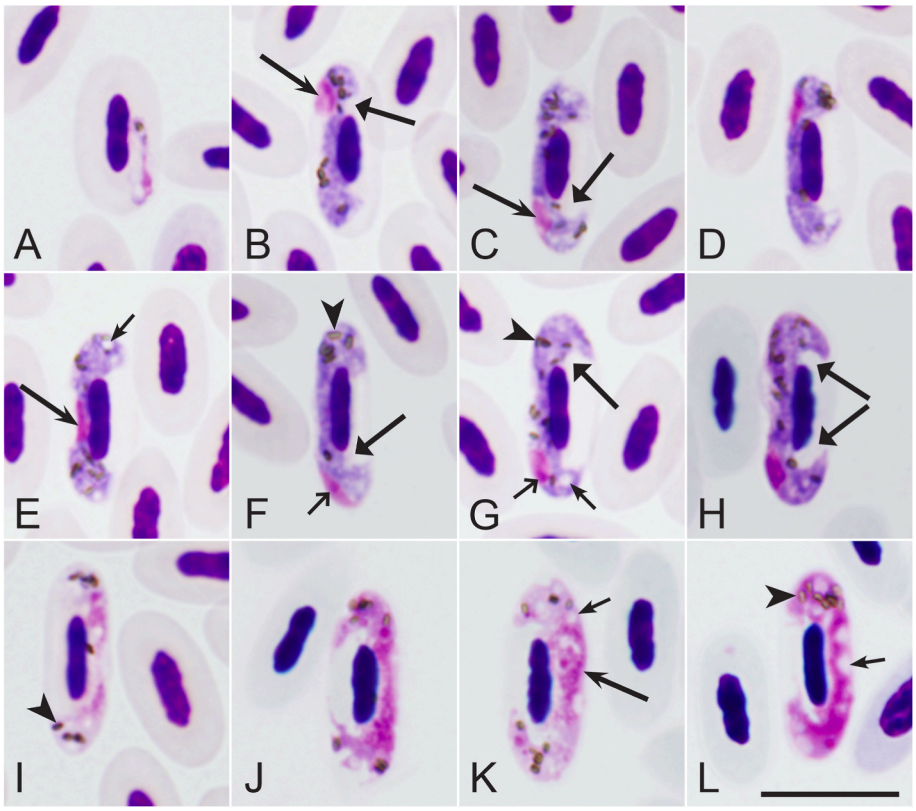

Fig. 2. Gametocytes of *Haemoproteus angustus* n. sp. (lineage hCWT7) from the blood of its type host, the common whitethroat *Curruca communis*: A-H – macrogametocytes, I-L – microgametocytes. Note: the markedly attenuated width of infected erythrocytes (D–G) containing advanced gametocytes, compared to uninfected erythrocytes, and the presence of predominantly oval or elongate pigment granules in fully grown gametocytes (F–H, J-L). All images are from the hapantotype. Long arrows – parasite nuclei. Short arrows – vacuoles. Arrowheads – pigment granules. Short simple wide arrow – nucleolus. Long triangle wide arrows – unfilled spaces between erythrocyte nuclei and gametocytes. Giemsa-stained thin blood films. Scale bar = 10 μm.

and F) or slightly angular (Fig. 2C, D, G, H, Fig. 3B) on the gametocyte ends, which often were pointed (Fig. 2G, H, Fig. 3B). The parasite nucleus is compact, variable in form, usually subterminal in position, possesses a visible nucleolus (Fig. 2F and G); only occasionally, the nuclei were observed in central position (Fig. 2E). Pigment granules are mostly uniform in form and size – a characteristic feature of this species; they were predominantly oval or elongate (Fig. 2B–F, G, Fig. 3B, Fig. 4A). Infected erythrocytes were distorted in comparison to uninfected erythrocytes – a characteristic developmental feature of this species (Table 1). Particularly, the infected erythrocytes and their nuclei were enlarged in length ($P < 0.001$ for both characters) but decreased in width ($P < 0.001$ for both characters); these features are readily visible when infected and uninfected erythrocytes locate close to each other (compare Fig. 2D–G, Fig. 3B).

Microgametocytes (Fig. 2I–L, 3C, D, 4B): The general configuration is as for macrogametocytes with the usual haemosporidian sexual dimorphic characters, which are the pale staining of the cytoplasm and the large diffuse centrally located nuclei; dumbbell-shaped microgametocytes were uncommon; the cytoplasm is often markedly vacuolated in fully grown microgametocytes (Fig. 2K, L, 3C); other characters were as for macrogametocytes.

Development in vitro (Fig. 5A–L): Gametogenesis and development of zygotes and ookinetes were studied in vitro at temperature of 18–21 °C. Within 1–3 min after the exposure of infected blood to air (EBA), mature gametocytes rounded up and escaped from the infected erythrocytes (Fig. 5A). This process was accompanied by the appearance of several (between 2 and 5) small (up to 1.5 μm in largest diameter) roundish residual bodies (Fig. 5A–C, E), which separated from the parasites before leaving the host cells (Fig. 5C). Noticeably, the residual bodies developed fast, and were distinguishable within 1 min EBA. They were seen free in solution as distinct bodies after rupture of the host cells. The exflagellation (Fig. 5F), free microgametes (Fig. 5G), macrogametes (Fig. 5D), and fertilization of macrogametes (Fig. 5H) were seen within 3 min after EBA. The zygotes were morphologically like macrogametes. The initial stages of ookinete differentiation were seen approximately 2 h after EBA, indicating a rapid ookinete transformation. At this time, a long finger-like outgrowth appeared, located tangentially to the main body of the parasite (Fig. 5I). As the ookinete developed, this outgrowth markedly extended and formed the anterior or apical end of the ookinete. On the opposite end of the medium differentiated ookinete, the accumulation of pigment granules was seen (Fig. 5J). In the fully grown ookinete, the pigment and adjacent part of cytoplasm eliminated as a residual body (Fig. 5K). At all stages of the differentiating ookinete, several distinct 'vacuoles' were usually seen in the cytoplasm (Fig. 5I–K), and they often persisted in fully differentiated ookinetes (Fig. 5L). The mature ookinetes were seen 6 h after EBA; they looked like elongate worm-like bodies (Fig. 5L). A few pigment granules were seen in some mature ookinetes. The morphometric parameters of gametes and ookinetes are given in Table 2.

Taxonomic remarks: *Haemoproteus angustus* n. sp. (Fig. 2, Fig. 3A–D, Fig. 4A, B) should be distinguished from the haemoproteids commonly parasitizing warbles of the Sylviidae (Valkiūnas, 2005; Valkiūnas and Iezhova, 2022), particularly the morphologically similar *Haemoproteus belopolskyi* (Fig. 3E–H), *Haemoproteus parabelopolskyi* (Fig. 3I–L); *Haemoproteus pallidulus* (Fig. 3M–P), *Haemoproteus homogeneae* (Fig. 3Q–T) and *Haemoproteus majoris* (Fig. 3U–X). These parasites can occur in co-infection. Gametocytes of the new species can be distinguished from all the latter parasites, particularly due to three readily recognizable characters. First, the presence of numerous fully grown gametocytes, which pull host cell nuclei inside (Fig. 2D–G, J), resulting in the big

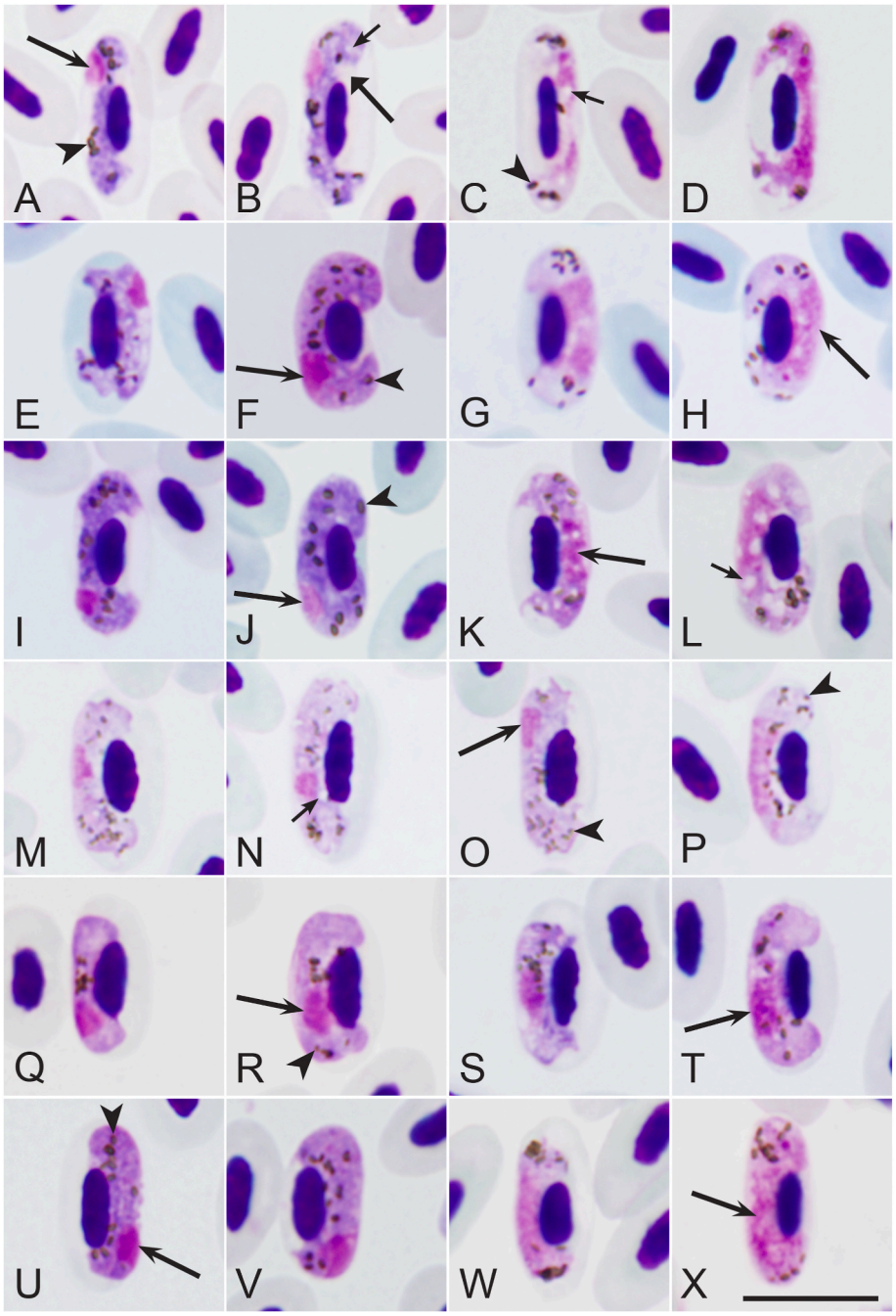

Fig. 3. Comparison of fully grown gametocytes of *Haemoproteus angustus* n. sp. (lineage hCWT7) from the blood of *Curruca communis* (A–D), *H. belopolskyi* (lineage hHIICT1) from the blood of *Hippolais icterina* (E–H) as well as *H. parabelopolskyi* (hSYAT2) (I–L), *H. pallidulus* (hSYAT3) (M–P), *H. homogeneae* (hSYAT16) (Q–T) and *H. majoris* (hWW2) (U–X) from the blood of *Sylvia atricapilla.* Note: the markedly attenuated gametocytes of the new species (A–D), which are not present in other *Haemoproteus* parasites (E–X); the fully grown gametocytes of *H. belopolskyi* (F, H) and *H. parabelopolskyi* (J, L) are bigger than those of *H. angustus* n. sp.; the pigment granules are predominantly roundish and small in *H. pallidulus* (M–P); the fully grown gametocytes are small and do not reach poles of infected erythrocytes in *H. homogeneae* (R, T); the erythrocyte nuclei are displaced laterally by *H. majoris* (V, X) – all these feature are not characteristic of *H. angustus* sp. nov. Symbols are the same as in Fig. 2. Giemsa-stained thin blood films. Scale bar = 10 μm.

value of nuclear displacement ratio (compare Fig. 3B–D with Fig. 3F–H, J, L, O, P, R, T, V, X). Second, the small width of the gametocytes (compare Fig. 3B–D with Fig. 3F–H, J, L, N, P, R, T, V, X). Thirdly, the thin fully grown macrogametocytes, which develop in erythrocytes that are atrophied in width (see Table 3). Additionally, the fully grown gametocytes of *H. belopolskyi* (Fig. 3F–H) and *H. parabelopolskyi* (Fig. 3J–L) are predominantly close to circumnuclear in form and can be even circumnuclear; the pigment granules are predominantly small (<0.5 μm) in *H. pallidulus* (Fig. 3O and P); the fully grown gametocytes of *H. homogeneae* are small and do not reach the poles of infected erythrocytes (Fig. 3R–T); the fully grown gametocytes of *H. majoris* markedly displace host cell nuclei laterally (Fig. 3V, X). None of these features are characters of *H. angustus* n. sp. (Fig. 2A–L, Fig. 3A–D, Fig. 4A, B).

Due to the big average NDR (≥1, see Table 1), *H. angustus* n. sp. (Fig. 4A and B) resembles *Haemoproteus dolniki* (Fig. 4C and D) and *Haemoproteus sittae* (Fig. 4E and F), parasites of passeriform birds (Valkiūnas, 2005). *Haemoproteus angustus* n. sp. (Fig. 4A and B) can be distinguished from these parasites due to the marked influence on the host cells nuclei, which are readily increased in length and decreased in

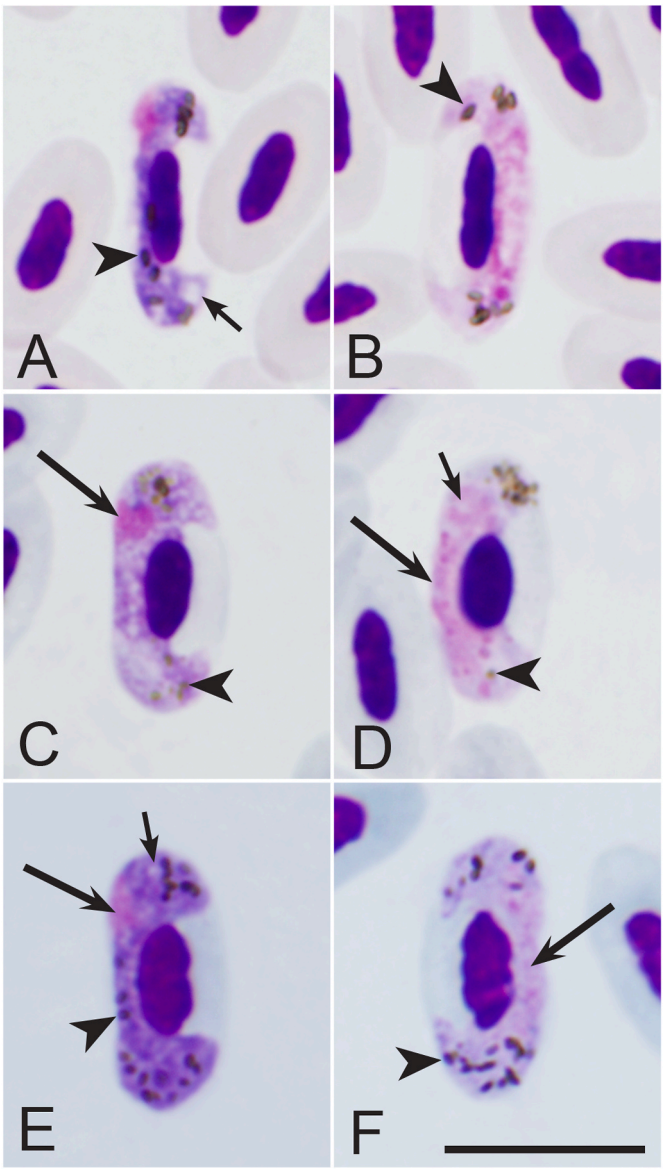

Fig. 4. Comparison of fully grown gametocytes of *Haemoproteus angustus* n. sp. (lineage hCWT7) from the blood of *Curruca communis* (A, B), *Haemoproteus sittae* (unknown lineage) from the blood of *Sittae europaea* (C, D) and *Haemoproteus dolniki* (unknown lineage) from the blood of *Fringilla coelebs* (E, F). Note: the elongate and markedly attenuated nuclei of infected erythrocytes containing advanced gametocytes of the new species (A, B), which is not the case in other *Haemoproteus* parasites (C–F). All images are from type specimens of these species. Symbols are the same as in Fig. 2. Giemsa-stained thin blood films. Scale bar = 10 μm.

width (Table 1); this is not the case in *H. dolniki* and *H. sittae* (compare Fig. 4A and B with Fig. 4C–F). Additionally, elongated pigment granules predominate in fully grown gametocytes of *H. angustus* n. sp. (Fig. 2, Fig. 3A–D, Fig. 4A) but not in *H. dolniki* or *H. sittae* (compare Fig. 4A and B with Fig. 4C–F).

The most closely related described species is *H. payevskyi* hRW01 (Fig. 1). Nuclei of microgametocytes of this parasite are markedly condensed (Valkiūnas and Iezhova, 2022), which is not the case in *Haemoproteus angustus* n. sp. (Fig. 2I–L). Due to development of the readily visible residual bodies during preparation of intracellular gametocytes for the gametogenesis (Fig. 5A–C, E), *H. angustus* is unique among currently investigated avian haemoproteids and thus can be readily distinguished at this stage of development in vitro.

Table 1
Morphometry of host cells and mature gametocytes of *Haemoproteus angustus* n. sp. (lineage hCWT7) from the blood of its type host the Common whitethroat *Curruca communis*.

Feature	Measurements (μm) [a]
Uninfected erythrocyte	
Length	10.2–12.0 (11.2 ± 0.4)
Width	5.2–6.5 (5.5 ± 0.3)
Area	43.5–61.0 (51.0 ± 3.8)
Uninfected erythrocyte nucleus	
Length	4.3–5.5 (4.9 ± 0.3)
Width	1.6–2.1 (1.8 ± 0.1)
Area	5.9–9.0 (7.6 ± 0.9)
Macrogametocyte	
Infected erythrocyte	
Length	12.0–13.9 (12.8 ± 0.6)
Width	4.5–5.8 (5.1 ± 0.4)
Area	47.6–60.7 (53.7 ± 3.9)
Infected erythrocyte nucleus	
Length	4.8–6.5 (5.6 ± 0.5)
Width	1.3–1.8 (1.5 ± 0.1)
Area	5.7–9.0 (7.5 ± 1.0)
Gametocyte	
Length	13.8–16.8 (15.3 ± 0.9)
Width	0.7–1.4 (1.0 ± 0.2)
Area	23.8–31.0 (27.2 ± 2.0)
Gametocyte nucleus	
Length	2.3–3.3 (2.8 ± 0.3)
Width	0.7–1.8 (1.3 ± 0.2)
Area	1.4–3.3 (2.6 ± 0.5)
Pigment granules#	6.0–13.0 (9.8 ± 1.8)
NDR [b]	0.9–1.3 (1.1 ± 0.1)
Microgametocyte	
Infected erythrocyte	
Length	13.3–15.1 (14.0 ± 0.5)
Width	4.6–6.8 (5.6 ± 0.5)
Area	56.7–76.2 (64.3 ± 5.0)
Infected erythrocyte nucleus	
Length	5.0–6.7 (6.0 ± 0.4)
Width	1.3–2.2 (1.6 ± 0.2)
Area	6.3–10.8 (8.3 ± 1.1)
Gametocyte	
Length	16.4–22.4 (18.8 ± 1.5)
Width	1.4–2.5 (2.0 ± 0.3)
Area	31.9–47.6 (40.0 ± 4.2)
Gametocyte nucleus	
Length	6.8–12.6 (9.5 ± 1.5)
Width	0.7–1.6 (1.2 ± 0.2)
Area	6.1–15.0 (10.2 ± 3.0)
Pigment granules	7.0–13.0 (9.3 ± 1.7)
NDR	0.8–1.3 (1.0 ± 1.1)

[a] All measurements (n = 21) are given in micrometers. Minimum and maximum values are provided, followed in parentheses by the arithmetic mean and standard deviation.

[b] NDR = nucleus displacement ration according to Bennett and Campbell (1972).

3.3. Host and geographical distribution

In the ML tree calculated with 1546 unique *Haemoproteus cytb* lineages, *H. angustus* hCWT7 and 20 similar *Haemoproteus* lineages formed a clade with maximum support (tree not shown). These lineages were predominantly found in *Curruca communis* and other members of the genus *Curruca* and differ from each other in a few bp only. A phylogenetic tree based on 478 bp *cytb* sequences of the 21 most closely related lineages is shown in Fig. 6A. A DNA haplotype network was calculated to visualize the distribution of these 21 lineages in bird hosts and geographic areas according to the UN geoscheme (Fig. 6B and C). The haplotype network includes three common lineages, hCWT7, hCWT2, and hCWT3, and 18 rare lineages, which were found in one or few individuals. Ten of these lineages, all of which were published by Drovetski et al. (2014) but not listed in the MalAvi database, were indicated by GenBank accession numbers instead of lineage names.

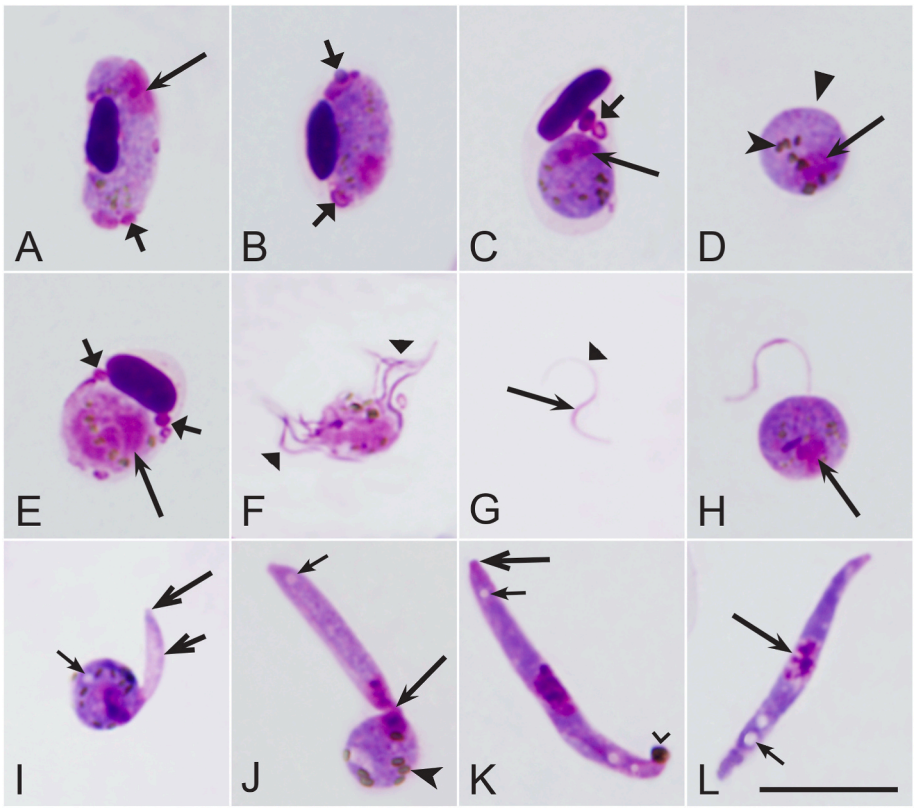

Fig. 5. *Haemoproteus angustus* n. sp. (lineage hCWT7) gametogenesis (A–H) and ookinete development (I–L) in vitro: A, B – initial stages of rounding up of gametocytes after the exposure of infected blood to air; C, E – rounded up macrogametocyte (C) and microgametocyte (E); F – the exflagellation; G – microgamete; H – fertilization; I – initial stage of ookinete development; J – medium differentiated ookinete; K – nearly mature ookinete with a residual body; L – mature ookinete without residual body. Note: the presence of several small residual bodies in erythrocytes containing gametocytes, which were preparing to escape from infected erythrocytes (A-C, E) – a unique character of this species during the initial stage of gametogenesis. Short triangle wide arrows – residual bodies; triangle arrowhead – macrogamete; triangle wide arrowheads – microgametes; short barbed arrows – finger-like outgrowth; long barbed arrows – apical end of developing ookinete; simple wide arrowhead – residual body of ookinete. Other symbols as in Fig. 2. Giemsa-stained thin blood films. Scale bar = 10 μm.

Table 2
Morphometric parameters of in vitro gametes and ookinetes of *Haemoproteus angustus* n. sp. (lineage hCWT7).

Feature	Measurements (μm)[a]
Macrogamete	
Length	5.8–7.8 (6.6 ± 0.6)
Width	3.8–6.7 (5.5 ± 0.8)
Area	22.1–38.6 (29.3 ± 5.2)
Microgamete	
Length	9.7–14.7 (12.4 ± 1.1)
Width	0.3–0.5 (0.4 ± 0.1)
Area	3.1–4.9 (3.8 ± 0.5)
Fully grown ookinete	
Length	18.1–22.4 (20.0 ± 1.1)
Width	1.3–2.8 (2.0 ± 0.4)
Area	20.7–40.0 (29.3 ± 5.0)

[a] All measurements (n = 21) are given in micrometers. Minimum and maximum values are provided, followed in parentheses by the arithmetic mean and standard deviation.

Lineage hCWT7 (32 records) was isolated from *C. communis* (29) in Turkey (19), Lithuania (3), Russia (2), Armenia (2), Sweden (1), Iran (1), and Botswana (1). Moreover, it was isolated from *Sylvia atricapilla* (1) and *Ficedula parva* (1) in Armenia and *Lanius collurio* (1) in Turkey, but there is no morphological confirmation about the presence of gametocytes of *H. angustus* n. sp. in bird species other than *C. communis*.

Lineage hCWT3 (34) was isolated from *C. communis* (22) in Turkey (14), Iran (2), Sweden (2), Armenia (1), Lithuania (1), Russia (1), and the UK (1). Moreover, it was isolated from *Curruca conspicillata* (10) in Cape Verde, *Sylvia atricapilla* (1) in Armenia, and *Sylvia borin* (1) in Nigeria.

Lineage hCWT2 (35) was isolated from *C. communis* (30) in Turkey (19), Armenia (4), Iran (2), Russia (2), Sweden (2), and Slovakia (1). Moreover, hCWT2 was isolated from *Sylvia borin* (2) in Russia and Nigeria, *S. atricapilla* (1) in Russia, and *Ficedula parva* (1) in Turkey.

Lineage hLWT1 (4) was isolated from *C. curruca* (3) in Nigeria (1), Turkey (1), and Slovakia (1), and *Curruca althaea* (1) in Iran, hSYNIS2

Table 3
Most readily recognizable morphometric differences between *Haemoproteus angustus* n. sp. and common haemoproteids parasitizing birds of the Sylviidae.

Haemoproteus species	Width of macrogametocytes	Width of erythrocytes infected with macrogametocytes	References
H. angustus	0.7–1.4 (1.0 ± 0.2)	4.5–5.8 (5.1 ± 0.4)	This study
H. belopolskyi	1.2–3.4 (2.4 ± 0.6)	6.7–7.8 (7.1 ± 0.2)	Valkiūnas (2005)
H. homogeneae	2.4–3.9 (3.0 ± 0.3)	6.2–8.0 (6.8 ± 0.4)	Valkiūnas et al. (2019)
H. majoris	1.8–3.2 (2.5 ± 0.4)	5.2–6.5 (5.5 ± 0.4)	Valkiūnas (2005)
H. pallidulus	1.4–2.5 (2.0 ± 0.2)	5.5–7.0 (6.3 ± 0.4)	Križanauskienė et al. (2010)
H. parabelopolskyi	1.2–2.6 (1.8 ± 0.3)	5.4–7.1 (6.1 ± 0.4)	Valkiūnas et al. (2007)

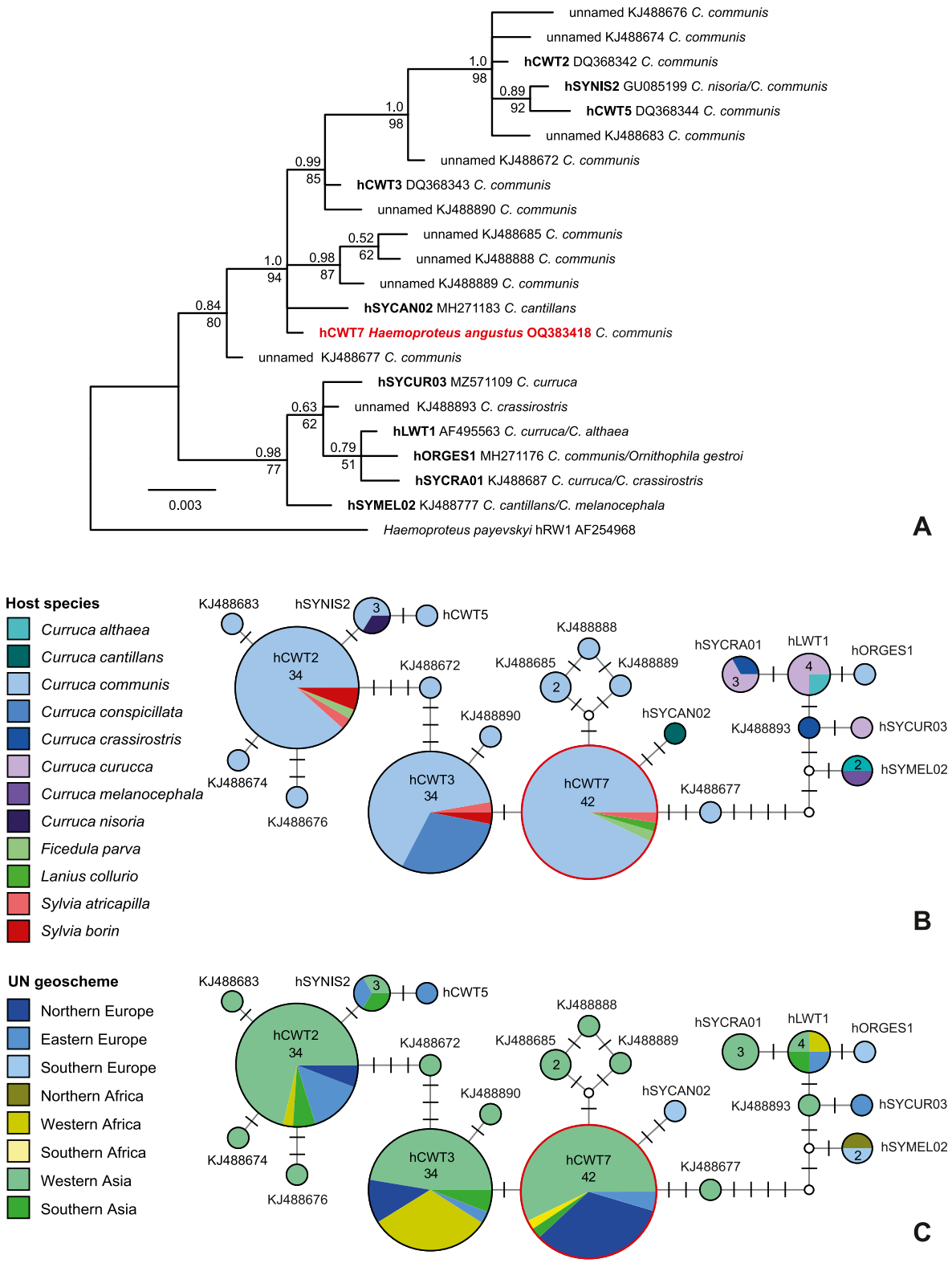

Fig. 6. Bayesian Inference tree (A) based on partial (478 bp) *cytb* sequences of *Haemoproteus angustus* n. sp. (lineage hCWT7) and the 20 closest related *Haemoproteus* lineages. Bayesian posterior probabilities and Maximum Likelihood bootstrap values were indicated above and below nodes, respectively. For each lineage, representative GenBank accession numbers and MalAvi lineage codes (if available) are indicated as well as the most common bird host. The scale bar indicates the expected mean number of substitutions per site according to the model of sequence evolution applied. Images B and C show the Median-Joining DNA haplotype network of partial (478 bp) *cytb* sequences of *H. angustus* hCWT7 and the 20 closest related *Haemoproteus* lineages. The upper image (B) shows the host distribution, and the lower image (C) depicts the geographic distribution according to the United Nations geoscheme. Each circle represents a unique haplotype/lineage. The frequency of each lineage is indicated for all haplotypes with more than one record and roughly corresponds to the size of circles. Bars on branches indicate the number of substitutions between two haplotypes. Small white circles represent median vectors, which are hypothetical (often ancestral or unsampled) sequences required to connect existing haplotypes with maximum parsimony.

(3) from *C. communis* (2) in Iran (1) and Turkey (1) and *C. nisoria* (1) in Bulgaria, hSYCRA01 (3) from *C. curruca* (2) and *Curruca crassirostris* (1) in Turkey, hSYMEL02 (2) from *Curruca cantillans* (1) in Morocco and *Curruca melanocephala* (1) in Italy, hCWT5 (1) from *C. communis* in Russia, hORGES1 (1) from *C. communis* in Spain, and hSYCUR03 (1) from *C. curruca* in Slovakia. Nine unnamed lineages (KJ488672, KJ488674, KJ488676, KJ488677, KJ488683, KJ488685, KJ488888-90) were isolated from one or two *C. communis* in Turkey, and one lineage (KJ488893) from *C. crassirostris* also in Turkey.

4. Discussion

This study highlights the following key findings, which are discussed below. First, the exo-erythrocytic development of *Haemoproteus* parasites can be undetectable during high gametocytaemia, even when using sensitive molecular diagnostic tools. Second, a unique feature of gametogenesis in haemosporidian parasites was reported, in particular the rapid formation of several residual bodies which separate from intracellular gametocytes before the formation of gametes. Third, the description and molecular characterization of a new *Haemoproteus* species, which predominantly infects a single avian species.

The damage of bird organs by exo-erythrocytic or tissue stages (meronts and megalomeronts) of *Haemoproteus* parasites was often mentioned as case reports published before 2000 (see reviews in Valkiūnas, 2005; Valkiūnas and Iezhova, 2017). However, due to common co-infection of different apicomplexan parasites in wildlife, it was unclear if the descriptions of these tissue stages truly belonged to *Haemoproteus* parasites. This was particularly uncertain in cases of megalomeronts, whose morphology (huge size, presence of capsular-like wall, lobular shapes) and location (gizzard, muscles) were unusual for haemosporidian parasites. In the absence of additional observations, haemosporidian experts tended to consider these as cases of aberrant leucocytozoonosis or even *Besnoitia* infections (Walker and Garnham, 1972; Bennett et al., 1993). Recent applications of PCR-based and CISH diagnostic methods have proved that *Haemoproteus* parasites produce enormously diverse tissue stages regarding both morphology and organ tropism (Ilgūnas et al., 2019; Duc et al., 2023a, 2023b; Himmel et al., 2024). While a few *Haemoproteus* species have been investigated in this regard, the patterns of exo-erythrocytic development – particularly the sequence of development and presence of meronts and megalomeronts in the life cycle – remain unclear. However, this knowledge is important for a better understanding of pathologies caused in avian hosts and the development of treatment measures. This is particularly true for recent discoveries of brain lesions associated with *Haemoproteus* infections (Duc et al., 2021, 2023a, 2023b; Himmel et al., 2024), which are the convincing descriptions of cerebral haemoproteosis, which was formerly known mainly for avian malaria in haemosporidians (Valkiūnas, 2005; Ilgūnas et al., 2016).

The development of research approaches aiming to access tissue stages during haemosporidian infections is needed. This is particularly true due to recent findings showing that records of the tissue stages are not necessarily correlated with the intensity of gametocytaemia during *Haemoproteus* infections. For example, the tissue stages might not be found during high parasitaemia but can be present at lower parasitaemia during *Haemoproteus* infections (Duc et al., 2021, 2023a, 2023b). In other words, parasitaemia intensity might not necessarily indicate active tissue development, and individuals with high parasitaemia might be less suitable candidates for exo-erythrocytic research. However, in previous studies, this observation was based on a limited number of birds and histological sections per individual examined. In the present study, seven infected birds with relatively high gametocytaemia were examined extensively – tens and even hundreds of HE-stained and CISH-treated histological sections were examined per bird individual – but tissue stages were not observed. Such extensive search for exo-erythrocytic stages combining traditional histology and CISH methods was done for the first time during avian haemosporidian research. The results were negative but are scientifically important, nevertheless. They show difficulties in research of exo-erythrocytic stages of *Haemoproteus* parasites in birds with intensive gametocytaemia even when sensitive molecular diagnostic methods are applied extensively.

The following explanation for the absence of tissue stages during high gametocytaemia is worth considering. Once infected with *Haemoproteus* parasites, birds can maintain infections for many years or even a lifespan (Valkiūnas, 2005). Due to the absence of erythrocytic merogony in haemoproteids, the persistence of *Haemoproteus* parasites in avian hosts is possible only by means of persisting tissue stages (Valkiūnas and Atkinson, 2020). The absence of detectable meronts and megalomeronts in tested birds suggests that tiny unicellular hypnozoite-like stages might be involved in the persistence of *Haemoproteus* infections, but such stages were not reported in avian haemoproteids thus far. Thus, this study calls for the application of additional diagnostic methods, e. g., immunohistochemistry and immunofluorescence in studies of life cycles of *Haemoproteus* species, as previously applied in the case of relapsing human *Plasmodium* species like *Plasmodium vivax* (Krotoski, 1989), or even more sensitive diagnostic tools, e. g. RNAscope in situ hybridization (Wang et al., 2012). Interestingly, it was suggested that hypnozoite-like tissue stages might exist in avian malaria parasites of the subgenus *Novyella* (Valkiūnas et al., 2016), however, there is still no convincing proof for that. The development of exo-erythrocytic merogony might be restricted to certain periods of the life cycle in some of *Haemoproteus* species. This calls for more targeted sampling of material for tissue stage research, which should involve infected birds of different ages, with varying levels of parasitaemia, and examined in different seasons.

It is worth noting that all birds investigated during this study were far-distance Afrotropical migrants sampled just after arrival to the study site from their wintering grounds in May. These birds must cross the Sahara Desert before reaching the sampling site (Snow and Perrins, 1998; Bensch and Åkesson, 2003), which is energy consuming (Dolnik, 1975). It might be that the disappearance of tissue stages in *Haemoproteus* parasites infecting far-distance migratory birds is an evolutionary adaptation minimizing the pathogenic effect due to lowering of the internal organ damage. This speculation is worth testing by examination of the same host-parasite associations in different seasons of the year, for example during wintering and breeding seasons, when tissue stages (meronts or megalomeronts) might appear due to possible hypnozoite-initiated relapses.

It should be mentioned that gametocytaemia was present in all examined birds, and the parasitaemia might be beneficial for the parasites during seasonal migration because it provides an opportunity for their transmission to vectors at bird stopover sites and thus, contribute to the spread of the parasites. Gametocytes of *H. angustus* were viable because they readily produced gametes (Fig. 5F) in vitro and the fertilization was visible (Fig. 5H). Moreover, ookinetes developed. It is interesting that the high parasitaemia in all histologically examined birds consisted of mature gametocytes (Fig. 7) indicating that meronts – the only possible source of merozoites, which initiate the development of gametocytes – might have already ruptured and thus were undetectable in organs. How to explain the presence of high gametocytaemia in case of non-detectable tissue stages? The limited experimental observations show that the maturation of *Haemoproteus* gametocytes takes approximately 3–4 days after infection of erythrocytes by merozoites, and gametocytes were still present in birds until the 11th day after the initial experimental infection (Ahmed and Mohammed, 1978), suggesting an opportunity of relatively long-lasting gametocyte persistence in circulation. In other words, the tissue stages might be cleared and the merozoites collectively entered erythrocytes, but the gametocytaemia still maintained due to occurrence of mature intracellular gametocytes. The long-time persistence of gametocytes in red blood cells is theoretically possible because the average lifespan of non-infected avian erythrocytes can be approximately a month (El-Mekawi et al., 1993),

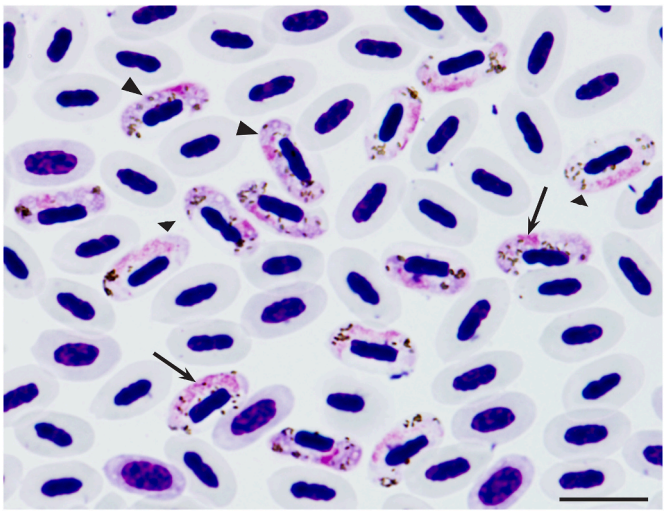

Fig. 7. High gametocytaemia of *Haemoproteus palloris* (lineage hWW1) from the blood of a willow warbler *Phylloscopus trochilus*. Note that young gametocytes are absent, and the parasitaemia consists exclusively of mature fully grown macro- and microgametocytes, indicating a synchronous parasite development and probable absence of recent maturation of tissue meronts, which are the only source of merozoites for young gametocyte development during *Haemoproteus* infections. Triangle arrowhead – macrogametocytes; triangle wide arrowheads – microgametocytes. Long arrows – parasite nuclei. Giemsa-stained preparations. Scale bar = 10 μm.

providing opportunities to gametocyte persistence in the circulation when exoerythrocytic merogony is reduced. Experimental observations are needed for a better understanding of this issue.

It is worth mentioning that Atkinson et al. (1986) reported the cellular infiltrates associated with the host immune response to degenerating megalomeronts and the remnants of degenerating myofibers up to 8 weeks after experimental infection of domestic turkeys with *Haemoproteus mansoni* (syn. H. *meleagridis*). Scar tissue was seen in muscles and indicated the past presence of megalomeronts. The presence of the scar tissues might be an additional indication of exo-erythrocytic development, but such tissue changes might go unnoticed by in situ hybridization. In our study, scar tissues were not seen during histological examinations. Nevertheless, it remains unclear whether the species in our study develop in muscle tissues or produce megalomeronts.

Another interesting observation of this study was the development of several tiny residual bodies during initial gametogenesis stages (Fig. 5A–C, E), reported for the first time in haemosporidian parasites. The bodies appeared rapidly and were visible inside infected erythrocytes already 1 min after EBA. The biological meaning of this phenomenon and the structure of the bodies remain unclear. The development of numerous species of avian *Haemoproteus* was investigated in vitro (Valkiūnas, 2005; Coral et al., 2015; Bukauskaitė et al., 2019), but residual bodies were seen only in *H. angustus* n. sp. It is worth mentioning that the diversity of wildlife haemosporidian parasites is huge and their life cycles remain insufficiently investigated. Many features are exclusive for life cycles of wildlife haemosporidians in contrast to haemosporidians infecting humans. For example, the exceptionally rapid (within 1 h at ambient temperature) maturation of *Haemoproteus* ookinetes and the tiny size (<10 μm) of the mature ookinetes; the presence of pedunculated oocysts in *Plasmodium juxtanucleare*, in which sporozoites gather at the periphery of oocysts before rupture; exceptionally rapid (within two days) maturation of oocysts in *Leucocytozoon (Akiba) caulleryi* at optimal sporogony conditions; remarkable enlargement of host cell nuclei in megalomeronts of *Leucocytozoon* sp.; the ability of *Plasmodium* merozoites to initiate merogony in various fixed and migrating cells, including leucocytes (Valkiūnas, 2005; Pendl et al., 2022). The molecular mechanisms of these unique haemosporidian features remain unknown. Surely, wildlife haemosporidians need much additional research to better understand the biology and evolution of the entire group of haemosporidian pathogens, which include human malaria parasites. This study shows that *H. angustus* n. sp. hCWT7 can be used as model organism for obtaining templates aiming at deeper molecular research on residual bodies during gametogenesis in haemosporidians. It is possible that other closely related lineages (Fig. 6A) could also be used for this purpose.

Gametocytes of *H. angustus* n. sp. were formerly observed during microscopic examination of birds belonging to the genus *Curruca*, but mainly in co-infection with other haemoproteids, which prevented a combined morphological and molecular characterization of this pathogen (TI and GV, personal observations). This study obtained the DNA barcode sequence of *H. angustus* n. sp. and linked it with morphological data, providing the opportunity to identify the species even during co-infections with morphologically similar parasites (see Taxonomic remarks). The available molecular data show that hCWT7 was most often recorded in Turkey (21 times) and Armenia (4) (Drovetski et al., 2014; MalAvi database, http://130.235.244.92/Malavi/index.html). Numerous bird blood samples were collected and analysed in Sweden, but the lineage hCWT7 was found only once (MalAvi database). Because there are no well-documented records of hCWT7 from juvenile birds in Europe, the lineage hCWT7 seems to be transmitted mainly in Western Asia or Africa at the birds' wintering sites, as is the case for *H. homopalloris* lineage hWW1, which is also mainly of Afrotropical transmission (Bensch and Åkesson, 2003; MalAvi database).

Phylogenetic analysis placed *H. angustus* n. sp. hCWT7 in a diverse group of haemoproteids, which belong to the subgenus *Parahaemoproteus* (Fig. 1, clades A–D), suggesting that this parasite is transmitted by *Culicoides* biting midges like many investigated species of the same clades (Chagas et al., 2018; Bukauskaitė et al., 2019). It is also worth mentioning that *H. angustus* n. sp. hCWT7 phylogenetically clustered with parasites, whose vertebrate hosts are exclusively passerine birds (Fig. 1, clade C). Generally, four provisional clades can be distinguished in the phylogenetic tree in regard of occupation of passerine and non-passerine birds. These include parasites, which complete development and produce gametocytes exclusively in non-passerine birds (Fig. 1, clades A, D), exclusively in passerine birds (Fig. 1, clade C), or in both passerine and non-passerine birds (Fig. 1, clade B). There is no convincing information supporting that some *Haemoproteus* species can complete their life cycle and produce gametocytes in birds of different orders (Valkiūnas, 2005; Valkiūnas and Atkinson, 2020). Thus, the available phylogenetic information provides an opportunity to speculate that closely related groups of *Haemoproteus* parasites have evolved different abilities to inhabit mainly non-passerines (Fig. 1, clades A, D), or passerines (Fig. 1, clade C), or both groups of these avian hosts (Fig. 1, clade B). More representative phylogenetic analyses using complete mitochondrial genomes and nuclear genes are needed to test this hypothesis, requiring further collection of genetic information, which remains insufficient for most species mentioned in Fig. 1. Nevertheless, recent studies showed that parasites which are closely related (cluster in well supported clades) based on the short *cytb* barcode fragment tend to display similar morphological features and parasitize birds of the same family. In other words, such phylogenetic information might be used to predict biological characters (for example, the vector preference – biting midges or louse flies – the rate of ookinete development and their size, some features of tissue merogony) (Valkiūnas et al., 2021; Duc et al., 2023a). The phylogenetic relationships are worthy of attention in parasitology research not only from an evolutionary point of view but also regarding practical parasitology research aiming to better understand parasite development.

This study specified new directions for future research using combined experimental, microscopy and molecular biology approaches for better understanding diversity and exo-erythrocytic development of wildlife haemosporidian parasites.

Declaration of Competing Interest

None.

Acknowledgements

V. Jusys and V. Eigirdas are acknowledged for assistance in bird catching and identification at Ventės Ragas Ornithological Station, Lithuania. This research was funded in part by the Research Council of Lithuania (RCL) [grants S-PD-22-71, S-MIP-23-2] and supported by the Open Access to research infrastructure of the Nature Research Centre under Lithuanian open access network initiative. This research was funded in part by the Austrian Science Fund (FWF) (grant P 33480). For the purpose of open access, the author has applied a CC BY public copyright licence to any Author Accepted Manuscript version arising from this submission.

References

Ahmed, F.E., Mohammed, A.-H., 1978. Studies of growth and development of gametocytes in *Haemoproteus columbae* Kruse. J. Protozool. 25, 174–177.

Atkinson, C.T., Greiner, E.C., Forrester, D.J., 1986. Pre-erythrocytic development and associated host responses to *Haemoproteus meleagridis* (Haemosporina: haemoproteidae) in experimentally infected domestic turkeys. J. Protozool. 33, 375–381. https://doi.org/10.1111/j.1550-7408.1986.tb05626.x.

Bennett, G.F., Campbell, A.G., 1972. Avian haemoproteidae. I. Description of *Haemoproteus fallisi* n. sp. and a review of the haemoproteids of the family Turdidae. Can. J. Zool. 50, 1269–1275. https://doi.org/10.1139/z72-172.

Bennett, G.F., Peirce, M.A., Ashford, R.W., 1993. Avian haematozoa: mortality and pathogenicity. J. Nat. Hist. 27, 993–1001. https://doi.org/10.1080/00222939300770621.

Bensch, S., Åkesson, S.J., 2003. Temporal and spatial variation of hematozoans in Scandinavian willow warblers. Parasitol 89, 388–391. https://doi.org/10.1645/0022-3395(2003)089[0388:TASVOH]2.0.CO;2.

Bensch, S., Stjernman, M., Hasselquist, D., Ostman, O., Hansson, B., Westerdahl, H., Pinheiro, R.T., 2000. Host specificity in avian blood parasites: a study of *Plasmodium* and *Haemoproteus* mitochondrial DNA amplified from birds. Proc. R. Soc. B. Biol. Sci. 267, 1583–1589, 1098/rspb.2000.1181.

Borst, G.H.A., Zwart, P., 1972. An aberrant form of *Leucocytozoon* infection in two quaker parakeets (*Myiopsitta monachus* Boddaert, 1783). Z. Parasitenkd. 40, 131–138.

Bukauskaitė, D., Iezhova, T.A., Ilgūnas, M., Valkiūnas, G., 2019. High susceptibility of the laboratory-reared biting midges *Culicoides nubeculosus* to *Haemoproteus* infections, with review on *Culicoides* species that transmit avian haemoproteids. Parasitology 146, 333–341. https://doi.org/10.1017/S0031182018001373.

Chagas, C.R.F., Bukauskaitė, D., Ilgūnas, M., Iezhova, T., Valkiūnas, G., 2018. A new blood parasite of leaf warblers: molecular characterization, phylogenetic relationships, description and identification of vectors. Parasit. Vectors 11, 538. https://doi.org/10.1186/s13071-018-3109-9.

Cococcetta, C., Zoller, G., Coutant, T., Luc, A.G., Duval, L., Huynh, M., 2023. Visceral *Haemoproteus minutus* infection in a major mitchell's cockatoo (*Lophochroa leadbeateri*). J. Avian Med. Surg. 37, 62–70. https://doi.org/10.1647/21-00026.

Coral, A.A., Valkiūnas, G., González, A.D., Matta, N.E., 2015. In vitro development of *Haemoproteus columbae* (Haemosporida: haemoproteidae), with perspectives for genomic studies of avian haemosporidian parasites. Exp. Parasitol. 157, 163–169. https://doi.org/10.1016/j.exppara.2015.08.003.

Darriba, D., Taboada, G.L., Doallo, R., Posada, D., 2012. JModelTest 2: more models, new heuristics and parallel computing. Nat. Methods 9, 772.

Dimitrov, D., Iezhova, T.A., Zehtindjiev, P., Bobeva, A., Ilieva, M., Kirilova, M., Bedev, K., Sjöholm, C., Valkiūnas, G., 2016. Molecular characterisation of three avian haemoproteids (Haemosporida, Haemoproteidae), with the description of *Haemoproteus* (*Parahaemoproteus) palloris* n. sp. Syst. Parasitol. 93, 431–449. https://doi.org/10.1007/s11230-016-9638-8.

Dolnik, V.R., 1975. The Migratory State of Birds. Nauka Publishers, Moscow (in Russian).

Drovetski, S.V., Aghayan, S.A., Mata, V.A., Lopes, R.J., Mode, N.A., Harvey, J.A., Voelker, G., 2014. Does the niche breadth or trade-off hypothesis explain the abundance–occupancy relationship in avian Haemosporidia? Mol. Ecol. 23, 3322–3329. https://doi.org/10.1111/mec.12744.

Duc, M., Himmel, T., Harl, J., Iezhova, T., Nedorost, N., Matt, J., Ilgūnas, M., Weissenböck, H., Valkiūnas, G., 2023a. Comparative analysis of the exo-erythrocytic development of five lineages of *Haemoproteus majoris*, a common haemosporidian parasite of European passeriform birds. Pathogens 12, 898. https://doi.org/10.3390/pathogens12070898.

Duc, M., Himmel, T., Ilgūnas, M., Eigirdas, V., Weissenböck, H., Valkiūnas, G., 2023b. Exo-erythrocytic development of two *Haemoproteus* species (Haemosporida, Haemoproteidae), with description of *Haemoproteus dumbbellus*, a new blood parasite of bunting birds (Emberizidae). Int. J. Parasitol. 53, 531–543. https://doi.org/10.1016/j.ijpara.2023.02.009.

Duc, M., Ilgūnas, M., Kubiliūnaitė, M., Valkiūnas, G., 2021. First report of *Haemoproteus* (Haemosporida, Haemoproteidae) megalomeronts in the brain of an avian host, with description of megalomerogony of *Haemoproteus pastoris*, the blood parasite of the Common starling. Animals 11. https://doi.org/10.3390/ani11102824.

Earlé, R.A., Bastianello, S.S., Bennett, G.F., Krecek, R.C., 1993. Histopathology and morphology of the tissue stages of *Haemoproteus columbae* causing mortality in Columbiformes. Avian Pathol. 22, 67–80. https://doi.org/10.1080/03079459308418901.

El-Mekawi, S., Yagil, R., Meyerstein, N., 1993. Effect of oxidative stress on avian erythrocytes. J. Basic Clin. Physiol. Pharmacol. 4, 199–211. https://doi.org/10.1515/jbcpp.1993.4.3.199.

Fowler, N.G., Forbes, G.B., 1972. Aberrant *Leucocytozoon* infection in parakeets. Vet. Rec. 91, 345–347.

Gardiner, C.H., Jenkins, H.J., Mahoney, K.S., 1984. Myositis and death in bobwhites, *Colinus virginianus* (L.), due to hemorrhagic cysts of a haemosporozoan of undetermined taxonomic status. J. Wildl. Dis. 20, 308–318.

Glez-Peña, D., Gómez-Blanco, D., Reboiro-Jato, M., Fdez-Riverola, F., Posada, D., 2010. ALTER: program-oriented conversion of DNA and protein alignments. Nucleic acids research 38 (Suppl. l_2), W14–W18.

Guindon, S., Gascuel, O., 2003. A simple, fast, and accurate algorithm to estimate large phylogenies by maximum likelihood. Syst. Biol. 52, 696–704. https://doi.org/10.1080/10635150390235520.

Hellgren, O., Krizanauskiene, A., Valkiūnas, G., Bensch, S., 2007. Diversity and phylogeny of mitochondrial cytochrome B lineages from six morphospecies of avian *Haemoproteus* (Haemosporida: haemoproteidae). J. Parasitol. 934, 889–896. https://doi.org/10.1645/GE-1051R1.1.

Hellgren, O., Waldenström, J., Bensch, S., 2004. A new PCR assay for simultaneous studies of *Leucocytozoon, Plasmodium*, and *Haemoproteus* from avian blood. J. Parasitol. 90, 797–802. https://doi.org/10.1645/GE-184R1.

Hernández-Lara, C., Duc, M., Ilgunas, M., Valkiūnas, G., 2021. Massive infection of lungs with exo-erythrocytic meronts in European Robin *Erithacus rubecula* during natural *Haemoproteus attenuatus* haemoproteosis. Animals 3273. https://doi.org/10.3390/ani11113273.

Himmel, T., Harl, J., Kübber-Heiss, A., Konicek, C., Fernández, N., Juan-Sallés, C., Ilgunas, M., Valkiūnas, G., Weissenböck, H., 2019. Molecular probes for the identification of avian *Haemoproteus* and *Leucocytozoon* parasites in tissue sections by chromogenic in situ hybridization. Parasit. Vectors 12, 1–10. https://doi.org/10.1186/s13071-019-3536-2.

Himmel, T., Harl, J., Matt, J., Nedorost, N., Lunardi, M., Ilgūnas, M., Iezhova, T., Valkiūnas, G., Weissenböck, H., 2024. Co-infecting *Haemoproteus* species (Haemosporida, Apicomplexa) show different host tissue tropism during exo-erythrocytic development in *Fringilla coelebs* (Fringillidae). Int. J. Parasitol. 54, 1–22. https://doi.org/10.1016/j.ijpara.2023.07.004.

Huelsenbeck, J.P., Ronquist, F., 2001. MRBAYES: Bayesian inference of phylogenetic trees. Bioinformatics 17, 754–755.

Ilgūnas, M., Bukauskaitė, D., Palinauskas, V., Iezhova, T.A., Dinhopl, N., Nedorost, N., Weissenbacher-Lang, C., Weissenböck, H., Valkiūnas, G., 2016. Mortality and pathology in birds due to *Plasmodium (Giovannolaia) homocircumflexum* infection, with emphasis on the exoerythrocytic development of avian malaria parasites. Malar. J. 15, 256. https://doi.org/10.1186/s12936-016-1310-x.

Ilgūnas, M., Chagas, C.R.F., Bukauskaitė, D., Bernotienė, R., Iezhova, T., Valkiūnas, G., 2019. The life cycle of the avian haemosporidian parasite *Haemoproteus majoris*, with emphasis on the exoerythrocytic and sporogonic development. Parasit. Vectors 12, 1–15. https://doi.org/10.1186/s13071-019-3773-4.

Katoh, K., Standley, D.M., 2013. MAFFT multiple sequence alignment software version 7: improvements in performance and usability. Mol. Biol. Evol. 30, 772–780. https://doi.org/10.1093/molbev/mst010.

Križanauskienė, A., Pérez-Tris, J., Palinauskas, V., Hellgren, O., Bensch, S., Valkiūnas, G., 2010. Molecular phylogenetic and morphological analysis of haemosporidian parasites (Haemosporida) in a naturally infected European songbird, the blackcap *Sylvia atricapilla,* with description of *Haemoproteus pallidulus* sp. nov. Parasitology 137, 217–227. https://doi.org/10.1017/S0031182009991235.

Krotoski, W.A., 1989. The hypnozoite and malarial relapse. Progr. Clin. Parasitol. 1, 1–19.

Nguyen, L.T., Schmidt, H.A., Von Haeseler, A., Minh, B.Q., 2015. IQ-TREE: a fast and effective stochastic algorithm for estimating maximum-likelihood phylogenies. Mol. Biol. Evol. 321, 268–274.

Ortiz-Catedral, L., Brunton, D., Stidworthy, M.F., Elsheikha, H.M., Pennycott, T., Schulze, C., Braun, M., Wink, M., Gerlach, H., Pendl, H., Gruber, A.D., Ewen, J., Pérez-Tris, J., Valkiunas, G., Olias, P., 2019. *Haemoproteus minutus* is highly virulent for Australasian and South American parrots. Parasit. Vectors 12, 1–10. https://doi.org/10.1186/s13071-018-3255-0.

Pendl, H., Hernández-Lara, C., Kubacki, J., Borel, N., Albini, S., Valkiūnas, G., 2022. Exo-erythrocytic development of *Plasmodium matutinum* (lineage pLINN1) in a naturally infected roadkill fieldfare *Turdus pilaris*. Malar. J. 21, 148. https://doi.org/10.1186/s12936-022-04166-x.

Sambrook, J., Russel, D.W., 2001. Molecular Cloning: A Laboratory Manual, third ed. Cold Spring Harbour Laboratory Press: Cold Spring Harbour, NY, USA.

Smith, G.A., 1972. Aberrant *Leucocytozoon* infection in parakeets. Vet. Rec. 91, 106.

Snow, D.W., Perrins, C.M., 1998. The Birds of the Western Palearctic. Oxford University Press, Oxford.

Svensson, L., 1992. Identification Guide to European Passerines, fourth ed. British Trust for Ornithology, Stockholm, p. 368.

Valkiūnas, G., 2005. Avian Malaria Parasites and Other Haemosporidia. CRC Press, Boca Raton, FL, USA.

Valkiūnas, G., Atkinson, C.T., 2020. Introduction to life cycles, taxonomy, distribution, and basic research techniques. In: Santiago-Alarcon, D., Marzal, A. (Eds.), Avian

Malaria and Related Parasites in the Tropics: Ecology, Evolution and Systematics. Springer Nature Switzerland AG, pp. 45–80.

Valkiūnas, G., Iezhova, T.A., 2017. Exo-erythrocytic development of avian malaria and related haemosporidian parasites. Malar. J. 16, 1–24. https://doi.org/10.1186/s12936-017-1746-7.

Valkiūnas, G., Iezhova, T.A., 2022. Keys to the avian *Haemoproteus* parasites (Haemosporida, haemoproteidae). Malar. J. 21, 269. https://doi.org/10.1186/s12936-022-04235-1.

Valkiūnas, G., Ilgūnas, M., Bukauskaitė, D., Chagas, C.R.F., Bernotienė, R., Himmel, T., Harl, J., Weissenböck, H., Iezhova, T., 2019. Molecular characterization of six widespread avian haemoproteids, with description of three new *Haemoproteus* species. Acta Trop. 197, 105051 https://doi.org/10.1016/j.actatropica.2019.105051.

Valkiūnas, G., Ilgūnas, M., Bukauskaitė, D., Duc, M., Iezhova, T.A., 2021. Description of *Haemoproteus asymmetricus* n. sp. (Haemoproteidae), with remarks on predictability of the DNA haplotype networks in haemosporidian parasite taxonomy research. Acta Trop. 218, 105905 https://doi.org/10.1016/j.actatropica.2021.105905.

Valkiūnas, G., Ilgūnas, M., Bukauskaitė, D., Žiegytė, R., Bernotienė, R., Jusys, V., Eigirdas, V., Fragner, K., Weissenböck, H., Iezhova, T.A., 2016. *Plasmodium delichoni* n. sp.: description, molecular characterisation and remarks on the exoerythrocytic merogony, persistence, vectors and transmission. Parasitol. Res. 1157, 2625–2636. https://doi.org/10.1007/s00436-016-5009-2.

Valkiūnas, G., Križanauskienė, A., Iezhova, T.A., Hellgren, O., Bensch, S., 2007. Molecular phylogenetic analysis of circumnuclear hemoproteids (Haemosporida: haemoproteidae) of sylviid birds, with a description of *Haemoproteus parabelopolskyi* sp. nov. J. Parasitol. 93, 680–687, 10./1645/GE-1102R.1.

Walker, D., Garnham, P.C.C., 1972. Aberrant *Leucocytozoon* infection in parakeets. Vet. Rec. 91, 70–72.

Wang, F., Flanagan, J., Su, N., Wang, L.C., Bui, S., Nielson, A., Wu, X., Vo, H.T., Ma, X.J., Luo, Y., 2012. RNAscope: a novel in situ RNA analysis platform for formalin-fixed, paraffin-embedded tissues. J. Mol. Diagn. 14, 22–29. https://doi.org/10.1016/j.jmoldx.2011.08.002.